This is the accepted manuscript made available via CHORUS. The article has been published as:

Gapless fermionic systems as phase-space topological insulators: Nonperturbative results from anomalies

Taylor L. Hughes and Yuxuan Wang

Phys. Rev. B **110**, L121119 — Published 23 September 2024

DOI: 10.1103/PhysRevB.110.L121119

Gapless Fermionic Systems as Phase-space Topological Insulators: Non-perturbative Results from Anomalies

Taylor L. Hughes[1] and Yuxuan Wang[2]

[1]*Department of Physics and Institute of Condensed Matter Theory, University of Illinois at Urbana-Champaign, Urbana, Illinois 61801-3080, USA*
[2]*Department of Physics, University of Florida, Gainesville, Florida 32611, USA*

(Dated: September 9, 2024)

We present a theory unifying the topological responses and anomalies of various gapless fermion systems exhibiting Fermi surfaces, including those with Berry phases, and nodal structures, which applies beyond non-interacting limit. As our key finding, we obtain a general approach to directly relate gapless fermions and topological insulators in phase space, including first- and higher-order insulators. Using this relation we show that the low-energy properties and response theories for gapless fermionic systems can be directly obtained without resorting to microscopic details. Our results provide a unified framework for describing such systems using well-developed theories from the study of topological phases of matter.

Introduction.— One of the most remarkable properties of topological insulators (TI) is their description in terms of quantized, detail-independent quantum anomalies [1, 2]. In contrast, spectral, thermodynamical, and transport properties of gapless systems such as Fermi liquids [3, 4] typically depend on the details of the dispersion and interactions. However, there are properties of interacting, gapless fermionic systems (GFSs) that are independent of microscopic details. Perhaps the most well-known example is Luttinger's theorem for a Fermi liquid [5–8], which is a non-perturbative result that relates the total electric charge with the volume enclosed by the Fermi surface.

Recently, it has been increasingly appreciated that Luttinger's theorem itself has a topological origin [7]—most directly, it follows from a topological Chern-Simons term in *phase space* (combining real and momentum space) [8, 9]. Indeed, phase-space topology has been utilized to classify gapped [1] and gapless [9, 10] fermionic systems having various internal symmetries. Additionally, the topological nature of Fermi surfaces even places important non-perturbative constraints on transport. [11] The power of phase space topology relies on an analogy between TIs with localized gapless excitations in position space, and GFSs with gapless modes localized on submanifolds of momentum space, e.g., Fermi surfaces or nodal lines/points.

While seminal work establishing this analogy was carried out in Refs. [8–10], in this work we obtain a general recipe for mapping GFSs to TIs in phase space. As a direct consequence of the phase-space approach, we obtain the low-energy properties, of both the bulk and the boundary, without relying on microscopic details. Importantly, such an approach yields a unified framework to understand a wide variety of GFSs including Fermi surfaces enclosing Berry phases and topological semimetals. From the quantum anomalies of the phase space TI, we unify various response theories for these GFSs and generate results that act as new types of Luttinger theorems that remain valid in the presence of interactions. Our work also sheds light on the classification of a variety of GFSs. [9, 12]

General Approach.— Our approach will be to associate a phase space TI (PSTI) having total phase-space dimension D (not counting time) to a given GFS. Then, we will use the known results of the topological response theories of TIs to describe properties of the GFS. [13] Let us denote the spatial dimension of the given GFS as d, and the co-dimension of the gapless-fermion submanifold in momentum space as c. While gapped in the "bulk," a PSTI has gapless modes on boundaries (or defects) having co-dimension C. While nontrivial surface states of first-order TIs correspond to $C = 1$, it is also known that TIs can host nontrivial gapless states on boundaries/defects having $C = 2$ (or larger values), such as in vortex cores, flux defects, [14] or the corners or hinges of a second-order TI. [15–33] The required dimension D of the PSTI can be determined via the following counting. We need d spatial dimensions, and also $d - c$ momentum coordinates to parameterize the gapless submanifold. In addition, we need C momentum coordinates to represent the "bulk" directions of the PSTI in momentum space. While the choice of the PSTI corresponding to a given GFS is not unique (i.e., the choice of C, and hence D is not unique), we find that the correspondence between a GFS and a PSTI can be described by the following general relation

$$D - C = 2d - c. \tag{1}$$

While the choice of D, C are not unique, there is a minimal case where C is chosen to be as small as possible. We list a few examples in Table I, and discuss several of them in detail below. As we will show, the topological response theory for PSTIs in the presence of the appropriate background gauge field configuration gives the correct description of the robust features of the GFS.

Let us note some immediate consequences of Eq. (1) for the classification of the stability of GFSs. It is

TABLE I. Examples for the correspondence between gapless fermionic systems and phase space TIs.

Gapless fermionic system	d	c	Phase space TI	D	C
1d Fermi surface	1	1	2d QHE	2	1
2d Fermi surface/doped Dirac semimetal [34]	2	1	4d QHE	4	1
2d Dirac semimetal	2	2	4d QHE/3d TI	4/3	2/1
3d Fermi surface/doped WSM	3	1	6d QHE	6	1
WSM_2	3	3	6d QHE/4d QHE	6/4	3/1
S_4-symmtric WSM	3	3	5d HOTI	5	2

well known from Ref. [14] that the topology of a *gapped* Hamiltonian is classified according to the difference between the position-space dimension d and its (effective) momentum-space dimension. For a boundary having co-dimension C in $(D-d)$-dimensional momentum-space, the effective momentum-space dimension for classification purposes is $(D-d)-(C-1)$ [14]. Hence, the classification of the PSTI and, via bulk-boundary correspondence, the GFS, depends only on, using Eq. (1), $d-[(D-d)-(C-1)]=c-1$, i.e., the classification depends only on the co-dimension of the gapless region of the GFS in momentum space, [9, 35] and is independent of the choice of D, C.

Fermi surfaces.— We begin by considering Fermi surfaces ($c=1$) of systems having spatial dimension $d=1$. As shown in Fig. 1(a), the minimal correspondence for a GFS in 1d is a Chern insulator in $D=2$ phase space where the 1d chiral Fermions at the Fermi surface (FS) can be regarded as edge states of the Chern insulator, i.e., edge states that are localized at a fixed momentum instead of a spatial boundary. The bulk phase-space theory that matches the chiral anomaly of the FS [35, 40] is given by

$$S=\frac{1}{4\pi}\int_{w,x,t}\mathcal{A}\wedge d\mathcal{A}, \tag{2}$$

where $w\sim k_x$, and $\mathcal{A}$ is the background gauge field in phase space. In particular, we expand the 1-form gauge field $\mathcal{A}$ as follows:

$$\mathcal{A}=eA+\mathfrak{a}+w\mathfrak{e}^{x}+w^2\mathfrak{e}^{xx}+w^3\mathfrak{e}^{xxx}+\cdots, \tag{3}$$

where A is the electromagnetic gauge field, $\mathfrak{e}^{abc\cdots}$ are the translation gauge field [43] and generalizations thereof, all of which have background values that live only in position space, and $\mathfrak{a}$ is the Berry connection, which, for our purposes, lives only in momentum space. Importantly, one needs to encode the information that some phase space coordinates, e.g., x and $w\sim k_x$, should not commute. This can be restored by adding a background gauge flux $F_{x,w}=1$ via a gauge choice $\mathcal{A}_x=w$, and projecting to an effective Landau level, analogous to noncommutative geometry emerging in quantum Hall physics. [41] Remarkably this immediately implies

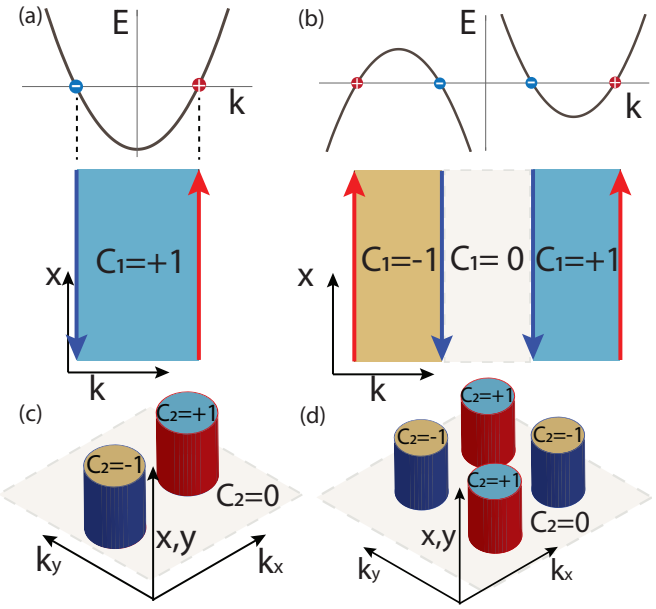


FIG. 1. Illustration of PSTIs corresponding to 1d FSs in (a),(b) and 2d FSs in (c), (d). Chern numbers $C_{1,2}$ with positive/negative signs correspond to electron/hole-like pockets. In (a), (b), $D=2, C=1, d=1, c=1$, and in (c), (d), $D=4, C=1, d=2, c=1$. As discussed in the text, in (b,c,d) the system has a vanishing (i.e., compensated) density and trivial Luttinger theorem relation, but satisfies additional generalized Luttinger theorems for higher powers of momentum.

that the translation gauge field has a background value $\mathfrak{e}^i_\mu=\delta^i_\mu$ stemming from the fundamental relation that momentum translates position. The background values for generalized translation gauge fields $\mathfrak{e}^{ab\cdots}$ are zero, but they may be turned on as probe fields.

Using this response action in the presence of the background configuration for $\mathfrak{e}^a$ immediately yields several non-perturbative results for various powers of the total momentum P_x (the zeroth power being the total particle

number N):

$$N = \int_{w,x} \frac{\delta S}{e\delta A_0} = \frac{1}{2\pi}\int dwdx\, \partial_w \mathcal{A}_x = \mathcal{P}\frac{L}{2\pi},$$
$$\langle P_x\rangle = \int_{w,x} \frac{\delta S}{\delta \mathfrak{e}_0^x} = \frac{1}{2\pi}\int dwdx\, w\partial_w \mathcal{A}_x = \frac{\mathcal{Q}}{2}\frac{L}{2\pi},$$
$$\langle P_x^2\rangle = \int_{w,x} \frac{\delta S}{\delta \mathfrak{e}_0^{xx}} = \frac{1}{2\pi}\int dwdx\, w^2\partial_w \mathcal{A}_x = \frac{\mathcal{O}}{3}\frac{L}{2\pi}, \quad (4)$$

where we have used $\mathfrak{e}_x^x = 1$ as a background value, and all other components of $\mathcal{A}$ are chosen to vanish. Here $\mathcal{P} = \int dw = \sum_a \chi_a k_F^{(a)}$ is the momentum-space dipole moment formed by all of the Fermi points $a = 1, 2, ...N_F$, where the χ_a are their chirality, and the $k_F^{(a)}$ are their corresponding Fermi momenta. The quantities $\mathcal{Q}$ and $\mathcal{O}$ are quadrupole and octupole moments of the Fermi points, which for a lattice system are only well-defined modulo the quanta of the contribution from a filled band, and (4) should be interpreted accordingly. For example, $\mathcal{P}$ is defined modulo $2\pi/a_0$, where a_0 is the lattice constant, and $\mathcal{Q}$ is defined modulo $2\pi/a \times 4\pi/L$. [42] Besides, any moment is gauge-invariant (i.e., invariant under a shift in momentum) only if all lower moments vanish. For example, this implies that $\mathcal{Q}$, and hence $\langle P_x\rangle$, is well-defined and independent of the origin of momentum space only if $\mathcal{P} = 0$ and $\chi = \sum_a \chi_a = 0$ as is the case for the configuration in Fig. 1(b). [43].

The first equation in (4) is simply the usual Luttinger theorem in 1d, while the subsequent equations are hierarchical generalizations of Luttinger's theorem that apply when each of the lower quantities vanish. For example, for a compensated semimetal that has a vanishing total density (which we can associate to a PSTI heterostructure as in Fig. 1(b)), our result predicts a relation between the total momentum and the quadrupole moment of the Fermi points. Furthermore, if the total momentum also vanishes, the total squared momentum is related to the octupole moment of the Fermi points, and so on. These results can be regarded as generalized Luttinger relations, relating short-distance quantities such as charge and momentum with the low-energy properties of the Fermi surfaces.

The generalized Luttinger theorems can be straightforwardly extended to higher dimensions. As an example, we can consider compensated semimetals in 2d having vanishing total density and broken or preserved inversion symmetry as shown in Fig. 1(c),(d) respectively. To be explicit, let us assume circular Fermi pockets with radius k_F centered at $(k_x, k_y) = (\pm K_x, 0)$ for Fig. 1(c), and around $(k_x, k_y) = (\pm K_x, \pm K_y)$ for Fig. 1(d). Both of these gapless systems can be understood as PSTIs having $D = 4$ according to Eq. (1) where $d = 2, c = 1, C = 1$. The $D = 4$ phase space is parameterized by $(w \sim k_x, v \sim k_y, x, y)$, where inside each electron or hole pocket we have a TI having a second Chern number $C_2 = \pm 1$ respectively. Indeed, in Ref. [9] the authors showed that the surface states of these 4D Chern insulators are the low-energy states near the 2d Fermi surfaces. The PSTI response theory is given by

$$S = \sum_{a=1}^{N_{\rm FS}} \frac{C_{2a}}{24\pi^2}\int_{(w,v)_a,x,y,t} \mathcal{A}\wedge d\mathcal{A}\wedge d\mathcal{A}, \quad (5)$$

where $N_{\rm FS}$ is the number of Fermi surface components and $C_{2a} = \pm 1$ is the second Chern number for each electron or hole pocket respectively. This action has been proposed to describe the LU(1) 't Hooft anomaly for a 2d Fermi liquid in Refs. [8, 44, 45], and analogous to Eq. (4), Eq. (5) straightforwardly leads to the 2d Luttinger theorem [9].

We can now show some additional consequences of this response by considering the FS's in Fig. 1(c) (Fig. 1(d)). The FS components are arranged in a dipolar (quadrupolar) pattern so we expect that the system will have a nonzero value of $\langle P_x\rangle$ ($\langle P_x P_y\rangle$). To extract this from the response we expand $\mathcal{A} = eA + w\mathfrak{e}^x + v\mathfrak{e}^y + w^2\mathfrak{e}^{xx} + v^2\mathfrak{e}^{yy} + vw\mathfrak{e}^{xy} + \cdots$ and perform the integrals in the w, v directions. We hence find the two expected responses for the dipolar and quadrupolar FS arrangements are captured by the following contributions to Eq. (5)

$$S_{\mathcal{P}} = \frac{\mathcal{P}_i V}{4\pi^2}\int_{x,y,t} \mathfrak{e}_0^i \mathfrak{e}_x^x \mathfrak{e}_y^y,\ S_{\mathcal{Q}} = \frac{\mathcal{Q}_{ij} V}{4\pi^2}\int_{x,y,t} \mathfrak{e}^{ij}\wedge\mathfrak{e}^x\wedge\mathfrak{e}^y, \quad (6)$$

where V is the volume of the system in position space, $\mathcal{P}_i = \sum_a \int C_{2a} k_i^{(a)} dk_x^{(a)} dk_y^{(a)}$ is the dipole moment of the Fermi pockets, and $\mathcal{Q}_{ij} = \sum_a \int C_{2a} k_i^{(a)} k_j^{(a)} dk_x^{(a)} dk_y^{(a)}$ is the quadrupole moment of the Fermi pockets. For the configuration in Fig. 1(c) $\mathcal{P}_x = 2K_x(\pi k_F^2)$, and for the configuration in Fig. 1(d) $\mathcal{Q}_{xy} = 2K_xK_y(\pi k_F^2)$, both of which are simply the 1d formulae for the Fermi-point dipole and quadrupole of the Fermi-pocket centers, but multiplied by the area of the Fermi pockets. The dipole $\mathcal{P}_x$ is unambiguously defined because the total density vanishes in Fig. 1(c), while $\mathcal{Q}_{xy}$ is well-defined because the density and $\mathcal{P}_i$ both vanish in Fig. 1(d). We thus have

$$\langle P_x\rangle = \int_{x,y} \frac{\delta S_{\mathcal{P}}}{\delta \mathfrak{e}_0^x} = \frac{V}{4\pi^2}\mathcal{P}_x, \quad (7)$$
$$\langle P_x P_y\rangle = \int_{x,y} \frac{\delta S_{\mathcal{Q}}}{\delta \mathfrak{e}_0^{xy}} = \frac{V}{4\pi^2}\mathcal{Q}_{xy}, \quad (8)$$

which are the 2d analogs of Eq. (4). If the system has C_4 or C_6 symmetry, $\mathcal{Q}$ has to vanish, and in that situation, the generalized Luttinger's theorem provides a non-perturbative relationship between expectation values of cubic powers of momentum and the octupole moment of the Fermi surface. We will discuss more details about these generalized Luttinger theorems in a future work [46].

FS's with Berry Phases.—The phase-space topological response theory can straightforwardly incorporate Berry phase effects in GFSs. Two important examples are the Fermi surfaces of a doped 2d Dirac semimetal, which enclose a π Berry phase, and the Fermi surfaces of a doped 3d Weyl semimetal (WSM) which enclose a Berry curvature monopole. We discuss the former in the Supplement [34], while here we consider a doped WSM having two spherical, hole-like FS's with radii $k_{F1} = k_{F2} \equiv k_F$ where each FS encloses a single Weyl point centered at $\vec{k}^{(a)}$ with chirality $\chi_a = \mp 1$, $a = 1, 2$. According to Eq. (1) (with $C = 1$), the corresponding PSTI to each WSM FS is a $D = 6$ Chern insulator parameterized by $(w \sim k_x, v \sim k_y, u \sim k_z, x, y, z)$, having a third Chern number $\mathcal{C}_3 = 1$ enclosing a vacuum region in the (w, v, u) subspace.

The $D = 6$ PSTI response action is given by [34]

$$S = \frac{1}{192\pi^3} \int_{w,v,u,x,y,z,t} \mathcal{A} \wedge d\mathcal{A} \wedge d\mathcal{A} \wedge d\mathcal{A}. \quad (9)$$

Keeping up to only linear couplings to momentum, we decompose the gauge field as $\mathcal{A} = eA + w\mathfrak{e}^x + v\mathfrak{e}^y + u\mathfrak{e}^z + \mathfrak{a}_m$, where $\mathfrak{a}_m$ is Berry connection created by the two monopoles in $\vec{k}$-space; over a surface enclosing one of the monopoles $\oint d\mathfrak{a}_m = \pm 2\pi$. The background configurations of the Berry monopole and the translation gauge fields generate the response theory up to quadratic order in A:

$$S = \int_{\mathbb{R}^4} \left[\frac{e\mathcal{V}}{8\pi^3} A \wedge \mathfrak{e}^x \wedge \mathfrak{e}^y \wedge \mathfrak{e}^z - \frac{e^2 \mathcal{P}_i}{8\pi^2} \mathfrak{e}^i \wedge A \wedge dA \right], \quad (10)$$

where $(t, x, y, z) \in \mathbb{R}^4$. The first term represents Luttinger's theorem in 3d, where $\mathcal{V}$ is the volume enclosed by the two FS's. [34] The second term is a response induced by $\mathfrak{a}_m$ describing the anomalous Hall effect $\sigma_{ij} = -\epsilon_{ijk} \frac{e^2}{4\pi^2} \mathcal{P}_k$. [40, 43] From Eq. (10) there also exists a momentum current response to the translation gauge field $\mathfrak{e}^i$ via $\mathfrak{j}_i^\mu \equiv \delta S / \delta \mathfrak{e}_\mu^i$, which carries the i-th component of momentum in the μ-th direction. The total momentum is $\langle P_i \rangle = \int_{\mathbb{R}^3} \star \mathfrak{j}_i$, and from Eq. (10) we obtain [34, 49]

$$\partial_t \langle P_i \rangle dt = \int_{\mathbb{R}^3} \left[\frac{e\mathcal{V}}{16\pi^3} \epsilon_{ijk} F \wedge \mathfrak{e}^j \wedge \mathfrak{e}^k - \frac{e^2 \mathcal{P}_i}{8\pi^2} F \wedge F \right], \quad (11)$$

where $F = dA$ is the background electromagnetic field. Using Luttinger's theorem, the coefficient of the first term in the second line of Eq. (11) is equal to the electric force eNE_i. The second term $\propto \vec{E} \cdot \vec{B}$ describes additional momentum generation via the chiral Landau levels (cLLs) of the Weyl fermions even at $\mathcal{V} = 0$. [50]

The same result (11) can be equivalently seen from an emergent anomaly of the PSTI boundary. To illustrate this connection, note that from the PSTI analogy, the gapless fermions on the a-th FS exhibit an emergent charge anomaly, given by $d \star j^{(a)}(\vec{k}_F^{(a)}) = \frac{e}{16\pi^3} F \wedge d(k_j \mathfrak{e}^j) \wedge d(k_l \mathfrak{e}^l) + \frac{e^2}{16\pi^3} F \wedge F \wedge \mathfrak{f}_m(\vec{k}_F^{(a)})$, [51] where $\mathfrak{f}_m = d\mathfrak{a}_m$ is the Berry curvature on the Fermi surface, and $\vec{k}_F^{(a)}$ is a Fermi momentum. The momentum current depends on the particle current and is given by $\mathfrak{j}_i^{(a)} \equiv \oint_{\mathrm{FS}_a} k_{F,i}^{(a)} j^{(a)}(\vec{k}_F^{(a)})$, and $\partial_t \langle P_i \rangle dt = \sum_a \int_{\mathbb{R}^3} d \star \mathfrak{j}_i^{(a)}$ evaluates to

$$\partial_t \langle P_i \rangle dt = \int_{\mathbb{R}^3} \frac{e\mathcal{V}}{16\pi^3} \epsilon_{ijl} F \wedge \mathfrak{e}^j \wedge \mathfrak{e}^l + \sum_a \oint_{\mathrm{FS}_a} k_{F,i}^{(a)} \frac{\mathfrak{f}_m(\vec{k}_F^{(a)})}{2\pi} \int_{\mathbb{R}^3} \frac{e^2}{8\pi^2} F \wedge F. \quad (12)$$

Matching (11) and (12) immediately leads to

$$\mathcal{P}_i = -\sum_a \oint_{\mathrm{FS}_a} k_{F,i}^{(a)} \frac{\mathfrak{f}_m(\vec{k}_F^{(a)})}{2\pi}, \quad (13)$$

which agrees with a direct bulk evaluation. [34] For linear dispersion around the FS this simplifies to $\mathcal{P}_i = \sum_{a=1}^2 \chi_a k_i^{(a)}$, i.e., the anomalous Hall effect σ_{ij} is proportional to the dipole moment of the Weyl points, independent of doping. The weak dependence on doping was first derived using a Green's function method [52]. From the general formula Eq. (13), $\mathcal{P}_i$ receives contributions from all FS points weighted by the Berry curvature. That the anomalous Hall effect in 3d is a FS phenomenon [53, 54] was first pointed out in Ref. [55], but compared with earlier works, our result is established non-perturbatively [56] from anomaly inflow. Additionally, the explicit inclusion of the translation gauge field captures the crystalline-electromagnetic response phenomena as well. [57–73]

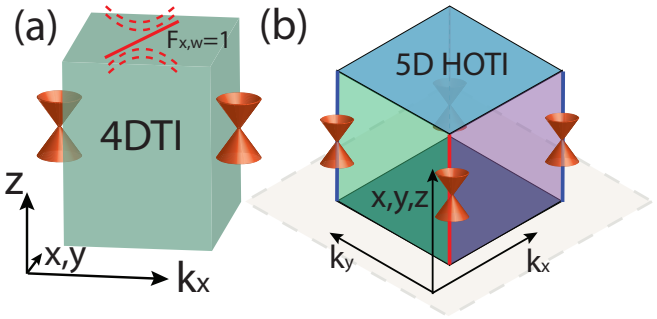


FIG. 2. Illustration of PSTIs for WSM_2 and S_4-symmetric WSM. In (a), $D = 4, C = 1, d = 3, c = 3$, and we see bulk Weyl nodes on the surfaces in the k_x direction while the z-surface modes are subjected to a phase space magnetic field $F_{x,w}$ that generates the Fermi arcs on the WSM surface. In (b), $D = 5, C = 2, d = 3, c = 3$, and bulk Weyl nodes appear on the hinges as domain wall states generated by opposing surface mass terms (purple and green masses have opposite signs). Weyl points on neighboring hinges have opposite chiralities.

Weyl semimetal.— As one shrinks the Fermi pockets to Weyl points, the first term in Eq. (10) vanishes, and we are left with the expected anomalous Hall response from

nodal Weyl points. In this nodal, semi-metallic limit, instead of including all three momentum coordinates, a simpler, alternative description of the WSM having two Weyl points (WSM_2) is constructed by viewing the Weyl points as surface states of a 4d Chern insulator as shown in Fig. 2(a). In this description, the phase space TI has dimension $D = 4$ and $C = 1$. For $\vec{k}^{(1,2)} = (\pm K_x, 0, 0)$, the "bulk" PSTI response action is described by [40]

$$S = \frac{1}{24\pi^2} \int_{w\in W,\mathbb{R}^4} \mathcal{A} \wedge d\mathcal{A} \wedge d\mathcal{A}, \tag{14}$$

where $w \sim k_x \in W \equiv [-K_x, K_x]$ separates the bulk two Weyl points. Together with the chiral anomaly from the "surface" Weyl fermions, and using the gauge field $\mathcal{A} = eA + w\mathfrak{e}^x$, Eq. (14) correctly produces the action (10) in the $\mathcal{V}_a = 0$ limit as expected.

As an advantage of the $D = 4$ description, one can easily take open boundary conditions in the y- and/or z-directions, since only the momentum direction w is needed in phase space. At a boundary having $z = z_0$, the 4d PSTI has surface states described by a 3d Weyl fermion: $H_{\text{surf}} = -i\int_{x,y,w} \psi^\dagger \left[(\partial_x - iw)\sigma_1 + \partial_y\sigma_2 + \partial_w\sigma_3\right]\psi$, where $w \in [-K_x, K_x]$, and the Weyl fermion is coupled to the background translational gauge field $\mathcal{A}_x = w$ (required to maintain the non-commutativity of x and k_x). As we mentioned, the canonical commutation relation in the x-direction is enforced when the spectrum is projected to the low-energy sector, which for Weyl fermions is the cLL. States in the cLL obey the eigenvalue constraint $\sigma_2\psi = \psi$, and the effective guiding-center constraint $\langle\partial_x - iw\rangle = 0$. Thus, projecting H_{surf} to the LLL we find $H = -i\int_{x,y} \tilde{\psi}^\dagger\partial_y\tilde{\psi}$, where $\langle i\partial_x\rangle = \langle w\rangle \in [-K_x, K_x]$. This Hamiltonian represents chiral dispersing surface modes having x-momenta restricted to $[-K_x, K_x]$, i.e., they describe the Fermi arc of a Weyl semimetal.

As we mentioned before, the PSTI description of GFS's is not unique. Indeed, both descriptions of the WSM (i) $D = 6, C = 3$ and (ii) $D = 4, C = 1$ satisfy Eq. (1) where $d = 3$ and $c = 3$. Since the classification of the phase space TI depends only on c, the two descriptions are equivalent, and are $\mathbb{Z}$-classified corresponding to the level of the Chern-Simons actions (9,14). It is well-known that the Chern number is stable even in the presence of interaction effects, and thus the $\mathbb{Z}$ classification applies to interacting systems [74], as long as translational symmetry is preserved, which is necessary for the definition of phase space and Weyl node separation. For example, it is known that no superconducting order parameter can gap out a WSM_2 (doped or not). [75] Furthermore, even when the Weyl points are gapped via topological order, the $\mathbb{Z}$ classification remains well-defined through the response theory. [76]

S_4-symmetric WSM.— Recent works have pointed out that more complicated Weyl-point configurations can have quasi-topological responses to electromagnetic and crystalline gauge fields [40, 43, 77]. As an example, we consider a WSM_4 having four Weyl nodes arranged in a quadrupolar pattern. Compared with previous works, we further impose a rotoinversion S_4 symemtry, which relates the four Weyl points. Interestingly, the corresponding PSTI is a higher-order TI (HOTI) where gapless states are localized at hinges where two surfaces intersect. We will show that the higher-order topology from the bulk has unique signatures for both the surface states and the response theory.

The phase-space coordinates of the HOTI are $(w, v, x, y, z) = (k_x, k_y, x, y, z)$, having surfaces at $w = \pm k_x^0, v = \pm k_y^0$, and hinges are located at $(w, v) = (\pm k_x^0, \pm k_y^0)$, as illustrated in Fig. 2(b). This HOTI can be constructed starting from a 5d PSTI that has massless 4d Dirac fermions on its surface and then subsequently gapping out the surface states with a spatially dependent mass term $m(w, v) = \mu(v^2 - w^2)$ that preserves S_4 [17]. The hinge states are hence domain wall states of 4d Dirac fermions, i.e., 3d Weyl fermions (bulk Weyl points) (see Fig. 2(b)).

The effective action of a 5d PSTI is given by [1] $S = \frac{\Theta}{48\pi^3}\int \mathcal{F}\wedge\mathcal{F}\wedge\mathcal{F}$, where $\Theta = \pi$, and a 5d HOTI with S_4 symmetry can be described by taking Θ to be varying (in phase space) as $\Theta = \pi\,\text{sgn}(v^2 - w^2) + \epsilon$, where $\epsilon \to 0$ [17]. This action is equivalent to Chern-Simons theories on the four side surfaces at $w = \pm k_x^0$ and $v = \pm k_y^0$, each of which has anomalous half-integer levels, i.e.,

$$S = \sum_{i=1}^{4} \frac{1}{2}\frac{1}{24\pi^2} \int_{\mathcal{S}_i\times\mathbb{R}^4} \text{sgn}(v^2 - w^2)\mathcal{A}\wedge d\mathcal{A}\wedge d\mathcal{A}, \tag{15}$$

where $\mathcal{S}_i$'s are the four boundaries in (w, v) forming a square connecting the four Weyl nodes.

As before the background gauge field configuration to leading order in momenta is given by $\mathcal{A} = eA + w\mathfrak{e}^x + v\mathfrak{e}^y$. Since the k-space dipole moment of the Weyl point vanishes, the lowest order response to the momentum gauge field is quadratic in momenta. We obtain

$$\begin{aligned} S =& \sum_{i=1}^{4} \frac{e}{2}\frac{(-1)^i}{8\pi^2} \int_{\mathcal{S}_i\times\mathbb{R}^4} d\left(k_\alpha\mathfrak{e}^\alpha\right)\wedge d\left(k_\beta\mathfrak{e}^\beta\right)\wedge A \\ =& \frac{e\mathcal{Q}_{\alpha\beta}}{8\pi^2}\int_{\mathbb{R}^4} \mathfrak{e}^\alpha\wedge d\mathfrak{e}^\beta\wedge A, \end{aligned} \tag{16}$$

where $\mathcal{Q}_{\alpha\beta}$ is the k-space quadrupole moment formed by the Weyl points. In our case $\mathcal{Q}_{xy} = \mathcal{Q}_{yx} = 4k_x^0k_y^0$. This is precisely the response theory in Refs. [40, 43] derived using other methods, which results in fractional charges bound at dislocations. Note that in the absence of S_4 symmetry, after integrating over momentum space there is in general another term in the action $\propto \mathfrak{e}^x\wedge\mathfrak{e}^y\wedge dA$, which corresponds to a non-vanishing charge polarization in the z-direction. While this term was omitted in previous works without justification, for the present system

its coefficient vanishes (modulo quantized contributions from filled bands) since it is odd under S_4.

The surface states for this system can also be directly obtained from phase-space topology. The top surface at $z = z_0$ is parameterized by (w, v, x, y) and harbors a 4d surface Dirac fermion subject to mass domain walls,

$$H_{\text{surf}} = -i \int_{w,v,x,y} \psi^\dagger \left[(\partial_x - iw)\Gamma_1 + (\partial_y - iv)\Gamma_2 + \partial_w \Gamma_3 + \partial_v \Gamma_4 + i\mu(v^2 - w^2)\Gamma_5 \right] \psi, \tag{17}$$

where $\{\Gamma_i\}$ are anticommuting Γ matrices with $\Gamma_5 = \Gamma_1\Gamma_2\Gamma_3\Gamma_4$, and we have added the background gauge field $\mathcal{A}_x = w$ and $\mathcal{A}_y = v$ to preserve the non-commutativity of x, k_x and y, k_y respectively. The two orthogonal phase-space magnetic fields allow us to project the Dirac fermion to the zeroth Landau level via $i\Gamma_1\Gamma_3\psi = i\Gamma_2\Gamma_4\psi = \psi$, and thus $\Gamma_5\psi = \psi$. Such a projection quenches the dispersion in the w, v directions and enforces the guiding center relations $\langle \partial_x - iw \rangle = \langle \partial_y - iv \rangle = 0$. The remaining mass term proportional to Γ^5 hence projects to $H = \mu \int_{x,y} \psi^\dagger (\partial_x^2 - \partial_y^2)\psi$, which forms crossing Fermi arcs connecting the four Weyl points. Interestingly, such a dispersion was recently shown to exhibit rank-2 chiral anomaly [77, 78], which can be canceled from the bulk using the response action we derived above.

Outlook.— We presented a unified framework of treating GFS's as phase-space TIs, leading naturally to non-perturbative results such as generalized Luttinger relations, topological response theories, and surface state properties. One immediate future direction is the classification of interacting GFS's from that of PSTIs [9]. It will also be interesting to extend this framework to GFSs with topological orders.

Acknowledgments.— We would like to thank Yi-Hsien Du, Lei Yang, and Chong Wang for useful discussions. YW is supported by NSF under award number DMR-2045781. TLH thanks ARO MURI W911NF2020166 for support. We acknowledge support by grant NSF PHY-1748958 to the Kavli Institute for Theoretical Physics (YW and TLH), and by grant NSF PHY-2210452 to the Aspen Center for Physics (YW), where this work was initiated and performed.

Notes added.— After submitting this manuscript to arXiv, we became aware of a related work by Wang and Sau [49] that was announced the same day.

[1] X.-L. Qi, T. L. Hughes, and S.-C. Zhang, Topological field theory of time-reversal invariant insulators, Phys. Rev. B **78**, 195424 (2008).
[2] E. Witten, Fermion path integrals and topological phases, Rev. Mod. Phys. **88**, 035001 (2016).
[3] R. Shankar, Renormalization-group approach to interacting fermions, Rev. Mod. Phys. **66**, 129 (1994).
[4] L. V. Delacrétaz, Y.-H. Du, U. Mehta, and D. T. Son, Nonlinear bosonization of fermi surfaces: The method of coadjoint orbits, Phys. Rev. Res. **4**, 033131 (2022).
[5] J. M. Luttinger, Fermi surface and some simple equilibrium properties of a system of interacting fermions, Phys. Rev. **119**, 1153 (1960).
[6] J. M. Luttinger and J. C. Ward, Ground-state energy of a many-fermion system. ii, Phys. Rev. **118**, 1417 (1960).
[7] M. Oshikawa, Topological approach to luttinger's theorem and the fermi surface of a kondo lattice, Phys. Rev. Lett. **84**, 3370 (2000).
[8] D. V. Else, R. Thorngren, and T. Senthil, Non-fermi liquids as ersatz fermi liquids: General constraints on compressible metals, Phys. Rev. X **11**, 021005 (2021).
[9] D.-C. Lu, J. Wang, and Y.-Z. You, Definition and classification of fermi surface anomalies (2023), arXiv:2302.12731 [cond-mat.str-el].
[10] D. Bulmash, P. Hosur, S.-C. Zhang, and X.-L. Qi, Unified topological response theory for gapped and gapless free fermions, Phys. Rev. X **5**, 021018 (2015).
[11] Z. D. Shi, H. Goldman, D. V. Else, and T. Senthil, Gifts from anomalies: Exact results for Landau phase transitions in metals, SciPost Phys. **13**, 102 (2022).
[12] P. Hořava, Stability of fermi surfaces and k theory, Phys. Rev. Lett. **95**, 016405 (2005).
[13] We emphasize that this correspondence is limited to their *topological* properties. For example, interactions in GFSs are nonlocal in k-space, leading to important differences with boundary states of (real-space) TIs. However, the topological properties are rooted in emergent quantum anomalies of the low-energy theory, which are robust against interactions [49].
[14] J. C. Y. Teo and C. L. Kane, Topological defects and gapless modes in insulators and superconductors, Phys. Rev. B **82**, 115120 (2010).
[15] W. A. Benalcazar, B. A. Bernevig, and T. L. Hughes, Quantized electric multipole insulators, Science **357**, 61 (2017).
[16] W. A. Benalcazar, B. A. Bernevig, and T. L. Hughes, Electric multipole moments, topological multipole moment pumping, and chiral hinge states in crystalline insulators, Phys. Rev. B **96**, 245115 (2017).
[17] F. Schindler, A. M. Cook, M. G. Vergniory, Z. Wang, S. S. P. Parkin, B. A. Bernevig, and T. Neupert, Higher-order topological insulators, Science Advances **4**, 10.1126/sciadv.aat0346 (2018).
[18] H. Shapourian, Y. Wang, and S. Ryu, Topological crystalline superconductivity and second-order topological superconductivity in nodal-loop materials, Phys. Rev. B **97**, 094508 (2018).
[19] J. Langbehn, Y. Peng, L. Trifunovic, F. von Oppen, and P. W. Brouwer, Reflection-symmetric second-order topological insulators and superconductors, Phys. Rev. Lett. **119**, 246401 (2017).
[20] L. Trifunovic and P. W. Brouwer, Higher-order bulk-boundary correspondence for topological crystalline phases, Phys. Rev. X **9**, 011012 (2019).
[21] E. Khalaf, Higher-order topological insulators and superconductors protected by inversion symmetry, Phys. Rev. B **97**, 205136 (2018).
[22] R.-X. Zhang, W. S. Cole, X. Wu, and S. Das Sarma, Higher-order topology and nodal topological superconductivity in fe(se,te) heterostructures, Phys. Rev. Lett. **123**, 167001 (2019).

[23] F. Liu, H.-Y. Deng, and K. Wakabayashi, Helical topological edge states in a quadrupole phase, Phys. Rev. Lett. **122**, 086804 (2019).

[24] Z. Yan, Majorana corner and hinge modes in second-order topological insulator/superconductor heterostructures, Phys. Rev. B **100**, 205406 (2019).

[25] Y. Xu, Z. Song, Z. Wang, H. Weng, and X. Dai, Higher-order topology of the axion insulator euin$_2$as$_2$, Phys. Rev. Lett. **122**, 256402 (2019).

[26] D. Călugăru, V. Juričić, and B. Roy, Higher-order topological phases: A general principle of construction, Phys. Rev. B **99**, 041301 (2019).

[27] Q. Wang, D. Wang, and Q.-H. Wang, Entanglement in a second-order topological insulator on a square lattice, EPL (Europhysics Letters) **124**, 50005 (2018).

[28] S. Franca, J. van den Brink, and I. C. Fulga, An anomalous higher-order topological insulator, Phys. Rev. B **98**, 201114 (2018).

[29] H. Li and K. Sun, Pfaffian formalism for higher-order topological insulators, Phys. Rev. Lett. **124**, 036401 (2020).

[30] P. Zhu, K. Loehr, and T. L. Hughes, Identifying C_n-symmetric higher-order topology and fractional corner charge using entanglement spectra, Phys. Rev. B **101**, 115140 (2020).

[31] M. Geier, L. Trifunovic, M. Hoskam, and P. W. Brouwer, Second-order topological insulators and superconductors with an order-two crystalline symmetry, Phys. Rev. B **97**, 205135 (2018).

[32] M. Ezawa, Higher-order topological insulators and semimetals on the breathing kagome and pyrochlore lattices, Phys. Rev. Lett. **120**, 026801 (2018).

[33] H. Fan, B. Xia, L. Tong, S. Zheng, and D. Yu, Elastic higher-order topological insulator with topologically protected corner states, Physical Review Letters **122**, 10.1103/physrevlett.122.204301 (2019).

[34] See the supplementary material.

[35] C. Wang, A. Hickey, X. Ying, and A. A. Burkov, Emergent anomalies and generalized luttinger theorems in metals and semimetals, Phys. Rev. B **104**, 235113 (2021).

[36] S. Ryu, A. P. Schnyder, A. Furusaki, and A. W. W. Ludwig, Topological insulators and superconductors: tenfold way and dimensional hierarchy, New Journal of Physics **12**, 065010 (2010).

[37] A. Kitaev, V. Lebedev, and M. Feigel'man, Periodic table for topological insulators and superconductors, in *AIP Conference Proceedings* (AIP, 2009).

[38] A. Kapustin, Symmetry protected topological phases, anomalies, and cobordisms: Beyond group cohomology (2014), arXiv:1403.1467 [cond-mat.str-el].

[39] A. Kapustin, R. Thorngren, A. Turzillo, and Z. Wang, Fermionic symmetry protected topological phases and cobordisms, Journal of High Energy Physics **2015**, 1–21 (2015).

[40] L. Gioia, C. Wang, and A. A. Burkov, Unquantized anomalies in topological semimetals, Phys. Rev. Res. **3**, 043067 (2021).

[41] J. Bellissard, A. van Elst, and H. Schulz-Baldes, The noncommutative geometry of the quantum hall effect, Journal of Mathematical Physics **35**, 5373–5451 (1994).

[42] The contribution to $\mathcal{Q}$ from a filled band is $(k_0 + 2\pi/a_0)^2 - k_0^2$, where $k_0 = 2\pi n_0/L$ is a lattice momentum. This contribution is an integer multiple of $2\pi/a \times 4\pi/L$.

[43] M. R. Hirsbrunner, O. Dubinkin, F. J. Burnell, and T. L. Hughes, Anomalous crystalline-electromagnetic responses in semimetals (2023), arXiv:2309.10840 [cond-mat.mes-hall].

[44] R. Ma and C. Wang, Emergent anomaly of fermi surfaces: a simple derivation from weyl fermions (2021), arXiv:2110.09492 [cond-mat.str-el].

[45] D. V. Else, Holographic models of non-fermi liquid metals revisited: an effective field theory approach (2023), arXiv:2307.02526 [cond-mat.str-el].

[46] Y. Wang and T. L. Hughes, in preparation.

[47] E. Witten, Dyons of charge $e\theta/2\pi$, Physics Letters B **86**, 283 (1979).

[48] S. Aoki, H. Fukaya, N. Kan, M. Koshino, and Y. Matsuki, Magnetic monopole becomes dyon in topological insulators, Phys. Rev. B **108**, 155104 (2023).

[49] S. Wang and J. D. Sau, Interaction robustness of the chiral anomaly in weyl semimetals and luttinger liquids from a mixed anomaly approach (2024), arXiv:2401.09409 [cond-mat.str-el].

[50] D. T. Son and B. Z. Spivak, Chiral anomaly and classical negative magnetoresistance of weyl metals, Phys. Rev. B **88**, 104412 (2013).

[51] By integrating over the FS, one obtains the chiral anomaly from the entire FS obtained in Ref. [79].

[52] A. A. Burkov, Anomalous hall effect in weyl metals, Phys. Rev. Lett. **113**, 187202 (2014).

[53] J.-Y. Chen and D. T. Son, Berry fermi liquid theory, Annals of Physics **377**, 345–386 (2017).

[54] X. Huang, Effective field theory of berry landau fermi liquid from the coadjoint orbit method (2023), arXiv:2312.00877 [cond-mat.str-el].

[55] F. D. M. Haldane, Berry curvature on the fermi surface: Anomalous hall effect as a topological fermi-liquid property, Phys. Rev. Lett. **93**, 206602 (2004).

[56] For interacting systems, the Berry curvature $\mathfrak{f}_m$ on the FS should be understood as defined via Green's functions [80, 81].

[57] M. R. Hirsbrunner, A. D. Gray, and T. L. Hughes, Crystalline-electromagnetic responses of higher order topological semimetals (2023), 2308.05796 [cond-mat.mes-hall].

[58] H. Sumiyoshi and S. Fujimoto, Torsional chiral magnetic effect in a weyl semimetal with a topological defect, Phys. Rev. Lett. **116**, 166601 (2016).

[59] K. Kodama and Y. Takane, Persistent current due to a screw dislocation in weyl semimetals: Role of one-dimensional chiral states, Journal of the Physical Society of Japan **88**, 054715 (2019), https://doi.org/10.7566/JPSJ.88.054715.

[60] Z.-M. Huang, L. Li, J. Zhou, and H.-H. Zhang, Torsional response and liouville anomaly in weyl semimetals with dislocations, Phys. Rev. B **99**, 155152 (2019).

[61] Z.-M. Huang, B. Han, and M. Stone, Nieh-yan anomaly: Torsional landau levels, central charge, and anomalous thermal hall effect, Phys. Rev. B **101**, 125201 (2020).

[62] L. Liang and T. Ojanen, Topological magnetotorsional effect in weyl semimetals, Phys. Rev. Research **2**, 022016 (2020).

[63] D. Pikulin, A. Chen, and M. Franz, Chiral anomaly from strain-induced gauge fields in dirac and weyl semimetals, Physical Review X **6**, 041021 (2016).

[64] Y. You, G. Y. Cho, and T. L. Hughes, Response properties of axion insulators and weyl semimetals driven by screw dislocations and dynamical axion strings, Physical

Review B **94**, 085102 (2016).
[65] R. Soto-Garrido, E. Muñoz, and V. Juričić, Dislocation defect as a bulk probe of monopole charge of multi-weyl semimetals, Phys. Rev. Res. **2**, 012043 (2020).
[66] S. Laurila and J. Nissinen, Torsional landau levels and geometric anomalies in condensed matter weyl systems, Phys. Rev. B **102**, 235163 (2020).
[67] J. Nissinen, T. T. Heikkilä, and G. E. Volovik, Topological polarization, dual invariants, and surface flat bands in crystalline insulators, Phys. Rev. B **103**, 245115 (2021).
[68] L.-L. Gao, S. Kaushik, D. E. Kharzeev, and E. J. Philip, Chiral kinetic theory of anomalous transport induced by torsion, Phys. Rev. B **104**, 064307 (2021).
[69] T. Amitani and Y. Nishida, Torsion-induced chiral magnetic current in equilibrium, Annals of Physics **448**, 169181 (2023).
[70] J. Nissinen and G. Volovik, Tetrads in solids: from elasticity theory to topological quantum hall systems and weyl fermions, Journal of Experimental and Theoretical Physics **127**, 948 (2018).
[71] J. Nissinen and G. Volovik, Elasticity tetrads, mixed axial-gravitational anomalies, and (3+ 1)-d quantum hall effect, Physical Review Research **1**, 023007 (2019).
[72] Y. Ferreiros, Y. Kedem, E. J. Bergholtz, and J. H. Bardarson, Mixed axial-torsional anomaly in weyl semimetals, Physical review letters **122**, 056601 (2019).
[73] C.-S. Chu and R.-X. Miao, Chiral current induced by torsional weyl anomaly, Physical Review B **107**, 205410 (2023).
[74] Here we focus on PSTI's without fractionalization. It would also be interesting to explore whether phase-space fractional topological insulators (PSFTI) can describe certain strongly correlated GFS.
[75] Y. Li and F. D. M. Haldane, Topological nodal cooper pairing in doped weyl metals, Phys. Rev. Lett. **120**, 067003 (2018).
[76] J. Yi, X. Ying, L. Gioia, and A. A. Burkov, Topological order in interacting semimetals, Phys. Rev. B **107**, 115147 (2023).
[77] O. Dubinkin, F. J. Burnell, and T. L. Hughes, Higher rank chiral fermions in 3d weyl semimetals (2021), arXiv:2102.08959 [cond-mat.mes-hall].
[78] P. Zhu, X.-Q. Sun, T. L. Hughes, and G. Bahl, Higher rank chirality and non-hermitian skin effect in a topolectrical circuit, Nat. Comms. **14**, 720 (2023).
[79] D. T. Son and N. Yamamoto, Berry curvature, triangle anomalies, and the chiral magnetic effect in fermi liquids, Physical Review Letters **109**, 10.1103/physrevlett.109.181602 (2012).
[80] C. Setty, F. Xie, S. Sur, L. Chen, S. Paschen, M. G. Vergniory, J. Cano, and Q. Si, Topological diagnosis of strongly correlated electron systems (2023), arXiv:2311.12031 [cond-mat.str-el].
[81] L. Peralta Gavensky, S. Sachdev, and N. Goldman, Connecting the many-body chern number to luttinger's theorem through středa's formula, Physical Review Letters **131**, 10.1103/physrevlett.131.236601 (2023).